Influence of Varying Temperature on Magneto hydrodynamics Peristaltic Flow of a Couple- Stress for a Jeffrey Fluid with Constant Viscosity through a Flexible Porous an inclined Channel

Saif Razzaq Mohsin Al-Waily[1], Zain Al-abdeen Abbas Al-safi[2] , Hala Abbas Mehdi[3] , Roaa Riyahd Hadi[4], Ahmed A.Hussein Al- Aridhee[5]

[1]Ministry of Education, Directorate of Najaf Education, Iraq, Email:saif.r.m.1993@gmail.com ,ma.post20@qu.edu.iq
[2]Wasit University, College, Computer Science and Information Technology, Iraq, Email: leccit3@uowasit.edu.iq
[3]Department of Mathematics, College of Science, University of Al-Qadisiyah, Diwaniya, Iraq, Email: halahaider2015@gmail.com
[4]Department of Mathematics, College of Computer Science and Information Technology, University of Al-Qadisiyah, Iraq, Email: Umarrush643@gmail.com
[5]Ministry of Education, Directorate of karbala Education, Iraq, Email: ahmedalardy845@gmail.com

Received: 17.04.2024 Revised : 18.05.2024 Accepted: 20.05.2024

ABSTRACT
Peristaltic motion of a Jeffrey fluid of constant viscosity and varying temperature across an inclined flexible tube with a porous channel. In this paper, Jeffrey fluid transmission was analyzed as well as the radially variable MHD was studied. The problem is formulated based on low Reynolds number and long wavelengths approximations. A parametric analysis was conducted to investigate the impact of (Darcy number; channel inclination angle; capacitance ratio; elasticity of channel walls). The flow lines show that the mundayemoves at the same speed as the wave and increases it. The study also showed that increasing the number of mundaye reduces the temperature.

Keywords:couple-stress flow, Jeffrey fluid, MHD,wall properties, porous channel

1. INTRODUCTION

The impact of flexible wall elasticity on non-Newtonian fluid MHD peristaltic flow in a porous channel. One kind of fluid transfer caused by a wave moving along a tube's walls is called peristalsis. It is a feature that many biological systems have by nature. First research on peristalsis was done in 1965 by Latham [1] (1966).The authors have employed dynamic boundary conditions to examine the elastic and viscoelastic properties of flexible borders and to consider the dynamic interplay between flexible and fluid walls, which is fundamental to peristalsis. This study aims to examine how MHD affects a couple's stress when they pass fluid via an inclined channel duct that is cylindrical and contains a porous medium. As of now, research has yet to explore the influence of a magnetic field and the impact of temperature variations on the flow of a Jeffrey liquid with couple's stress via a porous conduit with coordinates that are cylindrical. In [2]Study the elastic properties of the wall in general. [3] Calculated Nano fluid flow in an inclined channel with cross-sectional narrowing and permeability. Dealing with the peristaltic motion of a fluid using the law of power of particles in a tube with porous walls in [4]. [5]A couple's peristaltic motion is incompressible under tension. This article investigates the Jeffrey fluid's behavior in a cylindrical tube that is round and has elastic walls. For non-Newtonian fluids and pair stress, several publications have been published; see [6–10] for specifics.This study focuses on the peristaltic motion through a porous media inside a horizontal conduit of a Jeffrey fluid that is not Newtonian and has pair stress. A homogeneous magnetic field exerts strain on the unit [11].

2. Mathematical Formulation

A coaxial uniform circular pipe's incompressible Jeffrey fluid is strained in the event of a peristaltic pair. A non-Newtonian non-compressible fluid model known as the Jeffrey fluid represents the actual fluid in situations when shear stress and shear stress intensity (or velocity gradient) differ. Figure 1 illustrates

how to define the coordinates of a cylinder when Z is parallel to the pipe's axis and R is along the radius of the channel.

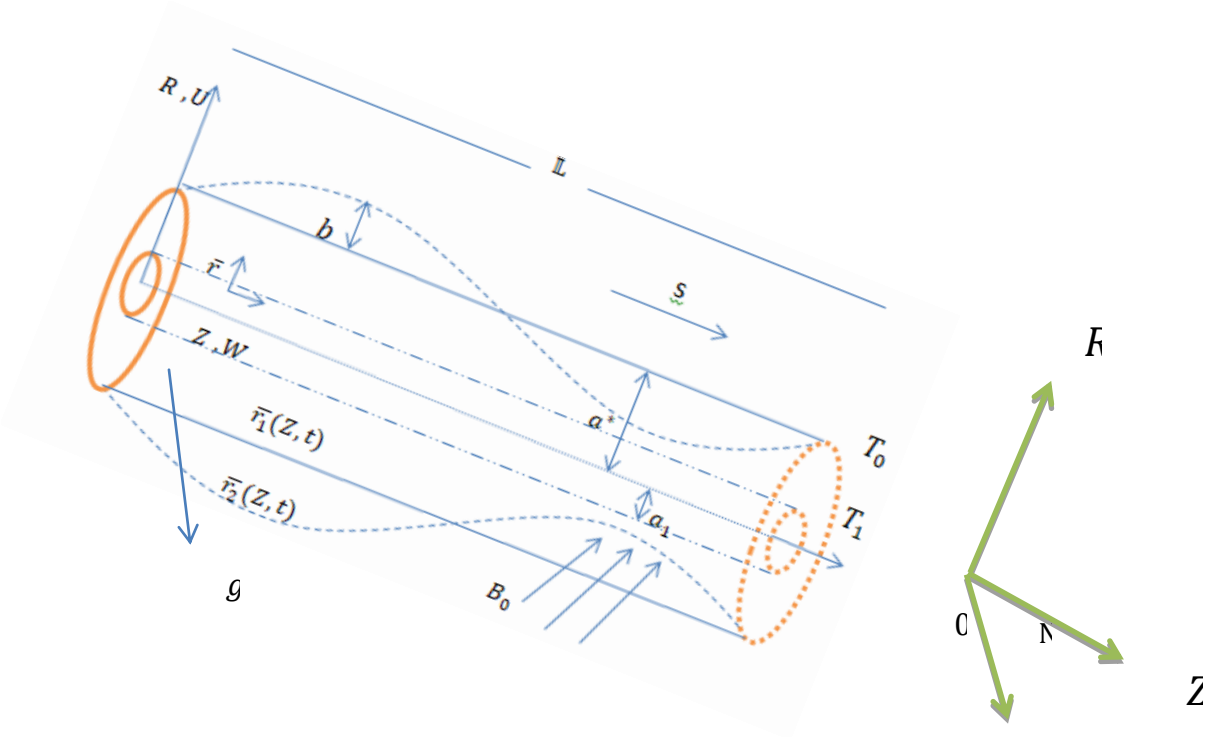

Graph 1: The geometry of the issue.

The configuration of the wall surface is delineated as:

$$\left.\begin{array}{l} \underline{r} = \underline{r_1} = a_1 \text{ Inner wall} \\ \underline{r} = \underline{\xi}(\underline{z},\underline{t}) = a^* + b\,\mathrm{Sin}\left(\frac{2\pi}{\mathbb{L}}(\underline{z} - s\underline{t})\right) \text{ Outer wall} \end{array}\right\} (1)$$

In this case, $a_1$represents the tube's undisturbed radius, a*represents the tube's disrupted radius,the peristaltic wave's amplitude was given by b,the wavelength was$\mathbb{L}$, the time was $\underline{t}$,andthe wave's speed of propagation was s.

2.1 Fundamental Equations

The following are the fundamental equations that govern:

Continuity equation ; $\nabla\underline{V} = 0$ (2)

The couple-stress fluid momentum equation is provided by;

$$\rho(\underline{V}.\nabla)\underline{V} = \nabla\underline{\sigma} + \mu_p\underline{J} \times \underline{B} - \frac{\mu}{K^*}\underline{V} + \rho g\beta_T(T - T_1)\sin(\ell) + \rho gN - \underline{\zeta}\nabla^4\underline{V} \quad (3)$$

The temperature equation is provided by;

$$T_s.\rho(\underline{V}.\nabla)T = T_c.\nabla^2 T - \nabla.Q_r - q(T - T_1). \quad (4)$$

where $\nabla^2 = \frac{1}{r}\frac{\partial}{\partial r}\left(r\frac{\partial}{\partial r}\right)$is the "Laplace operator" and $\nabla^4 = \nabla^2(\nabla^2)$. Also the velocity field is denoted by $\underline{V}$, ρ "density", μ "dynamic viscosity" temperature-dependent,k^* "permeability", We note that the flow is affected by the magnetic field in both the Z and R directions, J"current that is induced",$\underline{B} = (0,B_0^*\mathrm{Sin}(\ell),0)$is the inclination of fieldof magnetic,$\mu_p$the "magnetic permeability",$\underline{\sigma}$the "Cauchy stress tensor",$\underline{\zeta}$ is always associated with pair stress. Also T the "temperature and concentration", T_c is "thermal conductivity", T_s is "specific heat capacity" under steady pressure, ∇V the "fluid velocity gradient", $Q_r$the "radiation heat flux" and q "heat generation".

For an incompressible Jeffrey fluid, the constitutive equations are as follows:

$$\underline{\sigma} = -\underline{P}\underline{I} + \underline{S}, \quad (5)$$

$$\underline{S} = \frac{\mu}{1+\lambda_1}(\bar{\gamma} + \lambda_2\bar{\bar{\gamma}}). \quad (6)$$

where $\underline{S}$"extra stress tensor", $\underline{P}$ "pressure", $\underline{I}$"identity tensor", λ_1 "ratio of relaxation to retardation times", $\bar{\gamma}$" shear ratio", $\bar{\bar{\gamma}}$ "material derivative", and λ_2 "retardation time".

3. Solution Approach

In the stationary coordinates $(\underline{R}, \underline{Z})$, the flow between the two tubes is characterized by unsteadiness. It transitions into steadiness in a wave frame $(\underline{r},\underline{z})$ moving at the same velocity as the wave in the $\underline{Z}$-direction.The two frames' conversions are provided by;

$\underline{r} = \underline{R}\,, \underline{z} = \underline{Z}, \underline{u} = \underline{U}, \underline{w} = \underline{W} - s.$

where the components ofvelocity in the moving and stationary frames are indicated by (u, w) and (U, W). The motion equations that result from applying these transformations are;

$$\frac{\partial \underline{U}}{\partial \underline{R}} + \frac{\underline{U}}{\underline{R}} + \frac{\partial \underline{W}}{\partial \mathbf{Z}} = 0 \qquad (7)$$

$$\rho\left(\frac{\partial \underline{U}}{\partial \underline{t}} + \underline{U}\frac{\partial \underline{U}}{\partial \underline{R}} + \underline{W}\frac{\partial \underline{U}}{\partial \underline{Z}}\right) = -\frac{\partial \underline{p}}{\partial \underline{R}} + \frac{1}{\underline{R}}\frac{\partial}{\partial \underline{R}}\left(\underline{RS_{RR}}\right) + \frac{\partial}{\partial \underline{Z}}\left(\underline{S_{RZ}}\right) - \frac{\underline{S_{\vartheta\vartheta}}}{\underline{R}} - \frac{\mu}{k^*}\underline{U} - \rho g\cos(N) - \underline{\zeta\nabla^4 U} \quad (8)$$

$$\rho\left(\frac{\partial \underline{W}}{\partial \underline{t}} + \underline{U}\frac{\partial \underline{W}}{\partial \underline{R}} + \underline{W}\frac{\partial \underline{W}}{\partial \underline{Z}}\right) = -\frac{\partial \underline{p}}{\partial \underline{Z}} + \frac{1}{\underline{R}}\frac{\partial}{\partial \underline{R}}\left(\underline{RS_{RZ}}\right) + \frac{\partial}{\partial \underline{Z}}\left(\underline{S_{ZZ}}\right) + \rho g\beta_T(T - T_1)\sin(\ell) - \frac{\mu}{k^*}\underline{W} - \sigma\left(B_0^*\mathrm{Sin}(\ell)\right)^2\underline{W} + \rho g\sin(N) - \underline{\zeta\nabla^4 W} \qquad (9)$$

$$\frac{\partial T}{\partial \underline{t}} + \underline{U}\frac{\partial T}{\partial \underline{R}} + \underline{W}\frac{\partial T}{\partial \underline{Z}} = \frac{T_c}{T_s\rho}\left(\frac{\partial^2 T}{\partial \underline{R}^2} + \frac{1}{\underline{R}}\frac{\partial T}{\partial \underline{R}} + \frac{\partial^2 T}{\partial \underline{Z}^2}\right) - \frac{16\sigma_0 T_2^E}{3k_0 T_s\,\rho}\left(\frac{1}{\underline{R}}\frac{\partial T}{\partial \underline{R}} + \frac{\partial^2 T}{\partial \underline{R}^2}\right) - \frac{q}{T_s\,\rho}(T - T_1) \quad (10)$$

The corresponding boundary are;

$$\underline{w} = -1, \underline{u} = 0, T = T_2 \quad \text{at} \quad \underline{r} = \underline{r_1} = a_1,$$
$$\underline{w} = -1, \underline{u} = 0, T = T_1 \quad \text{at} \quad \underline{r} = \underline{\xi} = a^* + b\,\mathrm{Sin}\left(\frac{2\pi}{\mathbb{L}}(\underline{z} - s\underline{t})\right). \qquad (11)$$

The formula that determines the characteristics of a flexible wall channel is as follows;$\mathbb{F}$

$$\mathbb{F}^*\left(\underline{\xi}\right) = p - p_0 = \left(A\frac{\partial^4}{\partial \underline{z}^4} - N\frac{\partial^2}{\partial \underline{z}^2} + m\frac{\partial^2}{\partial \underline{t}^2} + C\frac{\partial}{\partial \underline{t}} + K_{\mathbb{F}}\right)\left(\underline{\xi}\right) \qquad (12)$$

where A represents the wall's flexural stiffness, Nstands for the length of tension per unit breadth, mstands for mass per unit area,$p_0$represents the pressure exerted by muscle tension on the outside wall surface,the spring stiffness is $K_{\mathbb{F}}$, and the viscous damping coefficient is C.

Administered the subsequent dimensionless changes as follows to streamline the motion's governing equations;

$$\left.\begin{aligned} u = \frac{\underline{u}\mathbb{L}}{a^* s}, w = \frac{\underline{w}}{s}, r = \frac{\underline{r}}{a^*},\ z = \frac{\underline{z}}{\mathbb{L}}, S = \frac{a^*\underline{s}}{\mu\, s}, \delta = \frac{a^*}{\mathbb{L}}, Da = \frac{k}{(a^*)^2}, t = \frac{\underline{st}}{\mathbb{L}}, \\ \mathbb{H} = \frac{T - T_1}{T_2 - T_1}, Rn = \frac{K_0 T_s \mu}{4T_2^E\sigma_0}, p = \frac{(a^*)^2 \underline{p}}{\mu s \mathbb{L}}, M^2 = \frac{\sigma(a^*)^2(B_0^*)^2}{\mu}\sin^2(\ell), Re = \frac{\rho s a^*}{\mu}, \underline{\nabla} = \frac{\nabla}{a^*} \\ r_1 = \frac{\underline{r_1}}{a^*} = \varepsilon < 1,\ \emptyset = \frac{b}{a^*},\ \xi = \frac{\underline{\xi}}{a^*} = 1 + \emptyset\sin(\underline{z} - s\underline{t}), t = \frac{\underline{st}}{\mathbb{L}}, F_r = \frac{s^2}{ga^*} \\ \alpha = \underline{\alpha}a^* = \sqrt{\frac{\mu}{\zeta}}a^*, Gr = \frac{\rho g\beta_T(a^*)^2(T_2 - T_1)}{\mu s}, Pr = \frac{\mu T_s}{T_c}, \Omega = \frac{q(a^*)^2}{\mu T_s} \end{aligned}\right\} \qquad (13)$$

where∅the "amplitude ratio", $\underline{\alpha}$ the "couple stress" fluid parameter indicating the ratio of the tube radius (constant) to material characteristic length ($\sqrt{\mu/\zeta}$, has the dimension of length),Re "Reynolds number", Pr"Prandtl number", Da "Darcy number",Rn "thermal radiation parameter", Gr "thermal Grashof number",M^2 "magnetic parameter", δthe "dimensionless wave number" and Ω "heat source/sink parameter"F_r the Froude number.

Rewriting the previous boundary conditions and governing equations in the following manner involves first introducing non-dimensional analysis (13) for equations (7) -(12) and then eliminating over-bars;

$$\left(\frac{s}{\mathbb{L}}\right)\left(\frac{\partial u}{\partial r} + \frac{u}{r} + \frac{\partial w}{\partial z}\right) = 0, \quad (14)$$

$$Re\,\delta^3\left(\frac{\partial u}{\partial t} + u\,\frac{\partial u}{\partial r} + (w + 1)\frac{\partial u}{\partial z}\right) = -\frac{\partial p}{\partial r} + \delta\frac{1}{r}\frac{\partial}{\partial r}(rS_{rr}) + \delta^2\frac{\partial}{\partial z}(S_{rz}) - \delta\frac{S_{\vartheta\vartheta}}{r} - \frac{\delta^2}{Da}u - \delta\frac{Re}{F_r}\cos(N) - \frac{\delta^2}{\alpha^2}\nabla^4 u \quad (15)$$

$$Re\,\delta\left(\frac{\partial w}{\partial t} + u\,\frac{\partial w}{\partial r} + (w + 1)\frac{\partial w}{\partial z}\right) = -\frac{\partial p}{\partial z} + \frac{1}{r}S_{rz} + \frac{\partial}{\partial r}(S_{rz}) + \delta\frac{\partial}{\partial z}(S_{zz}) - \left(M^2 + \frac{1}{D_a}\right)w + Gr\mathbb{H}\sin(\ell) - \left(M^2 + \frac{1}{D_a}\right) + \frac{Re}{F_r}\sin(N) - \frac{1}{\alpha^2}\nabla^4(w + 1) \quad (16)$$

$$Re\,\delta\left(\frac{\partial T}{\partial t} + u\,\frac{\partial \mathbb{H}}{\partial r} + (w + 1)\frac{\partial \mathbb{H}}{\partial z}\right) = \frac{1}{Pr}\left(\frac{\partial^2 \mathbb{H}}{\partial r^2} + \frac{1}{r}\frac{\partial \mathbb{H}}{\partial r} + \delta^2\frac{\partial^2 \mathbb{H}}{\partial z^2}\right) - \frac{4}{3Rn}\frac{1}{r}\frac{\partial}{\partial r}\left(r\frac{\partial \mathbb{H}}{\partial r}\right) - \Omega\mathbb{H} \quad (17)$$

Where

$$S_{rr} = \frac{2\delta}{1+\lambda_1}\left[1 + \frac{s\lambda_2\delta}{a^*}\left(\frac{\partial}{\partial t} + u\frac{\partial}{\partial r} + (w + 1)\frac{\partial}{\partial z}\right)\right]\left(\frac{\partial u}{\partial r}\right) \quad (18)$$

$$S_{rz} = \frac{1}{1+\lambda_1}\left[1 + \frac{s\lambda_2\delta}{a^*}\left(\frac{\partial}{\partial t} + u\frac{\partial}{\partial r} + (w + 1)\frac{\partial}{\partial z}\right)\right]\left(\frac{\partial w}{\partial r} + \delta^2\frac{\partial u}{\partial z}\right) \quad (19)$$

$$S_{\vartheta\vartheta} = \frac{2\delta}{1+\lambda_1}\left[\frac{u}{r} + \frac{s\lambda_2\delta}{a^*}\left(\frac{1}{r}\frac{\partial u}{\partial t} + \frac{u}{r}\frac{\partial u}{\partial r} - \frac{u^2}{r^2} + (w + 1)\frac{1}{r}\frac{\partial u}{\partial z}\right)\right] \quad (20)$$

$$S_{zz} = \frac{2\delta}{1+\lambda_1}\left[1 + \frac{s\lambda_2\delta}{a^*}\left(\frac{\partial}{\partial t} + u\frac{\partial}{\partial r} + (w + 1)\frac{\partial}{\partial z}\right)\right]\left(\frac{\partial w}{\partial z}\right) \qquad (21)$$

along with the appropriate dimensional boundary conditions are;

$$w=-1, u=0, \mathbb{H}=1 \quad at \quad r=r_1=\varepsilon,$$
$$w=-1, u=0, \mathbb{H}=0 \quad at \quad r=\xi=1+\emptyset\, Sin(2\pi(z-t)). \qquad (22)$$

The concept of continuity of stress states that the pressure at the fluid-wall interfaces must match the pressure acting on the fluid at $r=\xi$. At the complaint walls, the dynamic boundary conditions are obtained by using the z momentum equation.

$$\mathbb{F}_1\frac{\partial^5(\hbar)}{\partial z^5}-\mathbb{F}_2\frac{\partial^3(\hbar)}{\partial z^3}+\mathbb{F}_3\frac{\partial^3(\hbar)}{\partial z\,\partial t^2}+\mathbb{F}_4\frac{\partial^2(\hbar)}{\partial z\partial t}+\mathbb{F}_5\frac{\partial(\hbar)}{\partial z}=\frac{1}{r}S_{rz}+\frac{\partial}{\partial r}(S_{rz})-\left(M^2+\frac{1}{D_a}\right)w+Gr\mathbb{H}\,sin(\ell)-$$
$$\left(M^2+\frac{1}{D_a}\right)+\frac{Re}{F_r}sin(N)-\frac{1}{\alpha^2}\nabla^4(w+1) \qquad (23)$$

where $\mathbb{F}_1=\frac{A(a^*)^3}{\mu s\,\ell^5}$, $\mathbb{F}_2=-\frac{N(a^*)^3}{\mu s\,\ell^3}$, $\mathbb{F}_3=\frac{ms(a^*)^3}{\mu\ell^3}$, $\mathbb{F}_4=\frac{C(a^*)^3}{\mu\ell^2}$, and $\mathbb{F}_5=\frac{K_{\mathbb{F}}(a^*)^3}{\mu s\,\ell}$, whereas the wall's flexural stiffness is represented by $\mathbb{F}_1$, Length tension per unit width is expressed as $\mathbb{F}_2$, The mass in relation to area is $\mathbb{F}_3$, Viscosity damping coefficient is $\mathbb{F}_4$,correspondingly, $\mathbb{F}_5$ represents spring stiffness.

The analysis will be restricted to the supposition of a tiny dimensionless wave number ($\delta \ll 1$)as solving the problem in its extended form appears to be unachievable.But, we identified anestimated long wavelength. Equations (14)–(21) and (23) get the following from this supposition:

$$\frac{\partial u}{\partial r}+\frac{u}{r}+\frac{\partial w}{\partial z}=0 \qquad (24)$$
$$\frac{\partial p}{\partial r}=0 \qquad (25)$$
$$\frac{\partial p}{\partial z}=\frac{1}{r}(S_{rz})+\frac{\partial}{\partial r}(S_{rz})-\left(M^2+\frac{1}{D_a}\right)w+Gr\mathbb{H}\,sin(\ell)-\left(M^2+\frac{1}{D_a}\right)+\frac{Re}{F_r}sin(N)-\frac{1}{\alpha^2}\nabla^4(w+1) \qquad (26)$$
$$\left(\frac{1}{Pr}-\frac{4}{3Rn}\right)\left(\frac{\partial^2\mathbb{H}}{\partial r^2}+\frac{1}{r}\frac{\partial\mathbb{H}}{\partial r}\right)-\Omega\mathbb{H}=0 \qquad (27)$$

And

$$\mathbb{F}_1\frac{\partial^5(\hbar)}{\partial z^5}-\mathbb{F}_2\frac{\partial^3(\hbar)}{\partial z^3}+\mathbb{F}_3\frac{\partial^3(\hbar)}{\partial z\,\partial t^2}+\mathbb{F}_4\frac{\partial^2(\hbar)}{\partial z\partial t}+\mathbb{F}_5\frac{\partial(\hbar)}{\partial z}=\frac{1}{r}S_{rz}+\frac{\partial}{\partial r}(S_{rz})-\left(M^2+\frac{1}{D_a}\right)w+Gr\mathbb{H}\,sin(\ell)-$$
$$\left(M^2+\frac{1}{D_a}\right)+\frac{Re}{F_r}sin(N)-\frac{1}{\alpha^2}\nabla^4(w+1) \qquad (28)$$

where $S_{rr}=S_{\vartheta\vartheta}=S_{zz}=0$ and $S_{rz}=\frac{1}{1+\lambda_1}\left(\frac{\partial w}{\partial r}\right)$

Replacing S_{rz} into equation (28), we have:

$$\frac{1}{\alpha^2}\nabla^4 w-\frac{1}{1+\lambda_1}\frac{1}{r}\frac{\partial}{\partial r}\left(r\frac{\partial w}{\partial r}\right)+\left(M^2+\frac{1}{Da}\right)w=-\left(\mathbb{F}_1\frac{\partial^5(\hbar)}{\partial z^5}-\mathbb{F}_2\frac{\partial^3(\hbar)}{\partial z^3}+\mathbb{F}_3\frac{\partial^3(\hbar)}{\partial z\,\partial t^2}+\mathbb{F}_4\frac{\partial^2(\hbar)}{\partial z\partial t}+\mathbb{F}_5\frac{\partial\hbar}{\partial z}+\right.$$
$$\left.\left(M^2+\frac{1}{Da}\right)-\frac{Re}{F_r}sin(N)-Gr\mathbb{H}\,sin(\ell)\right) \qquad (29)$$

Given the assumption that the components of the pair stress tensor at the wall remain zero, the dimensionless boundary conditions that follow are as follows:

$$w=-1,\ \frac{\partial^2 w}{\partial r^2}-\frac{\alpha}{r}\frac{\partial w}{\partial r}=0 \quad at \quad r=\varepsilon,$$
$$w=-1,\ \frac{\partial^2 w}{\partial r^2}-\frac{\alpha}{r}\frac{\partial w}{\partial r}=0 \quad at \quad r=\xi. \qquad (30)$$

Where the parameter for the pair stress fluid is $\alpha=\frac{\mu}{\zeta}$, The pair stress is represented by the constants $\mu\to\zeta$, there is no pair stress effect when $\alpha\longrightarrow 1$ (i.e. $\mu\to\zeta$).

4. Solution for the problem

4.1 Equation for temperature

Rewrite equation (27) in the following manner;

$$r^2\frac{\partial^2\mathbb{H}}{\partial r^2}+r\frac{\partial\mathbb{H}}{\partial r}+Ar^2\mathbb{H}=0, \qquad (31)$$

where $A=-\frac{3\Omega PrRn}{3Rn-4Pr}$. A modification is made to equation (31) Bessel equation for 0th order. With boundary conditions $\mathbb{H}(r_1)=1, \mathbb{H}(\xi)=0$, the equation (31) may be solved as follows:

$$\mathbb{H}=B_1\,J_0[r\sqrt{A}]+B_2Y_0[r\sqrt{A}] \qquad (32)$$

Where $B_1=\frac{Y_0[\hbar\sqrt{A}]}{J_0[\epsilon\sqrt{A}]Y_0[\hbar\sqrt{A}]-J_0[\hbar\sqrt{A}]Y_0[\epsilon\sqrt{A}]}$ and $B_2=\frac{J_0[\hbar\sqrt{A}]}{J_0[\hbar\sqrt{A}]Y_0[\epsilon\sqrt{A}]-J_0[\epsilon\sqrt{A}]Y_0[\hbar\sqrt{A}]}$.

4.2 Equation of momentum

The momentum equation (29) should be rewritten as follows;

$$\nabla^4 w-\frac{\alpha^2}{1+\lambda_1}\left(\frac{1}{r}\frac{\partial}{\partial r}+\frac{\partial^2}{\partial r^2}\right)w+\alpha^2\left(M^2+\frac{1}{D_a}\right)w=-\alpha^2\left(\mathbb{F}_1\frac{\partial^5(\hbar)}{\partial z^5}-\mathbb{F}_2\frac{\partial^3(\hbar)}{\partial z^3}+\mathbb{F}_3\frac{\partial^3(\hbar)}{\partial z\,\partial t^2}+\mathbb{F}_4\frac{\partial^2(\hbar)}{\partial z\partial t}+\mathbb{F}_5\frac{\partial\hbar}{\partial z}+\right.$$
$$\left.\left(M^2+\frac{1}{D_a}\right)-\frac{Re}{F_r}sin(N)-Gr\mathbb{H}\,sin(\ell)\right) \qquad (33)$$

Set $2c_1=\frac{\alpha^2}{(1+\lambda_1)}$, $\mathscr{b}^4=\alpha^2\left(M^2+\frac{1}{D_a}\right)$.

The general solution of(33) is;

$$w = B_1 I_0\left(\mathscr{b} r\sqrt{|s_1|}\right) + B_2 K_0\left(\mathscr{b} r\sqrt{|s_1|}\right) + B_3 I_0\left(\mathscr{b} r\sqrt{|s_2|}\right) + B_4 K_0\left(\mathscr{b} r\sqrt{|s_2|}\right) - \frac{1}{M^2 + \frac{1}{D_a}}\left(\begin{matrix}\mathbb{F}_1(32\pi^5 \emptyset\, Cos[2\pi(z-t)]) - \mathbb{F}_2(-8\pi^3 \emptyset\, Cos[2\pi(z-t)]) + \mathbb{F}_3(-8\pi^3 \emptyset\, Cos[2\pi(z-t)]) + \\ \mathbb{F}_4(4\pi^2 \emptyset\, Sin[2\pi(z-t)]) + \mathbb{F}_5(2\pi\, \emptyset\, Cos[2\pi(z-t)]) + \left(M^2 + \frac{1}{D_a}\right) - \frac{Re}{F_r} sin(N) - Gr\mathbb{H}\, sin(\ell)\end{matrix}\right) \quad (34)$$

where $\mathscr{b}^4 = \alpha^2\left(M^2 + \frac{1}{D_a}\right)$,$s_1 = -\frac{c_1}{\mathscr{b}^2} - \sqrt{\left(\frac{c_1}{\mathscr{b}^2}\right)^2 - 1}$, $s_2 = -\frac{c_1}{\mathscr{b}^2} + \sqrt{\left(\frac{c_1}{\mathscr{b}^2}\right)^2 - 1}$ and $c_1 = \frac{\alpha^2}{2(1+\lambda_1)}$ with condition $\frac{c_1}{\mathscr{b}^2} > 1$. Additionally, the first and second kinds of modified Bessel functions of zero order are denoted by I_0 andK_0. The constants B_1, B_2, B_3 and B_4 may be obtained by using boundary conditions (30) and the Mathematica12 program.

4.3 Function of stream.

The stream's associated functions($u = -\frac{1}{r}\frac{\partial \psi}{\partial z}$ and $w = \frac{1}{r}\frac{\partial \psi}{\partial r}$) is;

$$\psi = \int r\left\{B_1 I_0\left(\mathscr{b} r\sqrt{|s_1|}\right) + B_2 K_0\left(\mathscr{b} r\sqrt{|s_1|}\right) + B_3 I_0\left(\mathscr{b} r\sqrt{|s_2|}\right) + B_4 K_0\left(\mathscr{b} r\sqrt{|s_2|}\right) - \frac{1}{M^2 + \frac{1}{D_a}}\left(\begin{matrix}\mathbb{F}_1(32\pi^5 \emptyset\, Cos[2\pi(z-t)]) - \mathbb{F}_2(-8\pi^3 \emptyset\, Cos[2\pi(z-t)]) + \mathbb{F}_3(-8\pi^3 \emptyset\, Cos[2\pi(z-t)]) + \\ \mathbb{F}_4(4\pi^2 \emptyset\, Sin[2\pi(z-t)]) + \mathbb{F}_5(2\pi\, \emptyset\, Cos[2\pi(z-t)]) + \left(M^2 + \frac{1}{D_a}\right) - \frac{Re}{F_r} sin(N) - Gr\mathbb{H}\, sin(\ell)\end{matrix}\right)\right\} dr$$

So that

$$\psi = \frac{r^2}{2}\left(\frac{\mathbb{F}_1(32\pi^5 \emptyset\, Cos[2\pi(z-t)]) - \mathbb{F}_2(-8\pi^3 \emptyset\, Cos[2\pi(z-t)]) + \mathbb{F}_3(-8\pi^3 \emptyset\, Cos[2\pi(z-t)]) + \mathbb{F}_4(4\pi^2 \emptyset\, Sin[2\pi(z-t)]) + \mathbb{F}_5(2\pi\, \emptyset\, Cos[2\pi(z-t)]) + \left(M^2 + \frac{1}{D_a}\right) - \frac{Re}{F_r} sin(N) - Gr\mathbb{H}\, sin(\ell)}{\left(M^2 + \frac{1}{D_a}\right)^2}\right) - \frac{B_2 r K_1\left(r\mathscr{b}\sqrt{|s_1|}\right)}{\mathscr{b}\sqrt{|s_1|}} - \frac{B_4 r K_1\left(r\mathscr{b}\sqrt{|s_2|}\right)}{\mathscr{b}\sqrt{|s_2|}} + \frac{1}{2} B_1 r^2\ {}_0\tilde{F}_1\ \left[2; \frac{r^2(\mathscr{b}\sqrt{|s_1|})^2}{4}\right] + \frac{1}{2} B_3 r^2\ {}_0\tilde{F}_1\ \left[2; \frac{r^2(\mathscr{b}\sqrt{|s_2|})^2}{4}\right] \quad (35)$$

where K_1represents the function of modified Besselof the second type and (${}_0\tilde{F}_1$) representsthe function of regular hypergeometric.

5. RESULTS AND DISCUSSION

Diagrams are provided in this section that illustrate the findings of both the numerical analysis as well as the computational analysis of the problem of the peristaltic motion of an elastic porous tube with elastic wall properties where Jeffrey fluids are incompressible to couple stresses. Additionally, it explores the effects of magnetic field and temperature on the velocity equation, along with their impacts on the wall of channel. Figure 1 depicts the geometry of a peristaltic flow pattern. The peristaltic flow of pair stress fluid across the elastic porous material in depicts 2-45 was interpreted by us using the Mathematics12 package.

5.1 Distribution of Temperature

Based on equation (32), figures 2-7 depict the influence of parameters Ω, ε, ∅, Rn,t, and Pr on the fluid temperature function $\mathbb{H}$ versus r.The fluid's temperature increases as the parameters ε, t, and Pr increase, as seen in Figures 2, 5, and 7,On the other hand, Figures 3, 4, and 6 show that as Rn, Ω, and ∅ are increased, a fluid's temperature drops.

5.2 Distribution of Velocity

Based on equation (34), figures 8-28 illustrate the effects of parameters ε, ∅, λ_1, $\mathbb{F}_5$, $\mathbb{F}_4$,$\mathbb{F}_3$, $\mathbb{F}_1$, t, $\mathbb{F}_2$, Da, α, ζ, U, Gr, Ω, Pr, Rn, Re, Fr, ϱ, and Σ on the velocity distribution w versus r.

The impact of the factors ε on the distribution ofvelocity of w against r is seen in Figure 8. It has been observed that the velocity w rises as ε grows at r>0.12, but w decreases as ε increases at r<0.12.Figures 9, 11, 12, 14, 16, 17, 18, 26, 27 and 28,As we increase ∅, $\mathbb{F}_5$, $\mathbb{F}_4$, $\mathbb{F}_1$, $\mathbb{F}_2$, Da, α, Fr, ϱ, and Σ, we observe the rotation of the effect of the parameters ∅, $\mathbb{F}_5$, $\mathbb{F}_4$, $\mathbb{F}_1$, $\mathbb{F}_2$, Da, α, Fr, ϱ, and Σ; that is, the velocity increases in the region r<0.2 and decreases with increasing ∅, $\mathbb{F}_5$, $\mathbb{F}_4$, $\mathbb{F}_1$, $\mathbb{F}_2$, Da, α, Gr, Re, and ϱ in the region r>0.2.Figures 8, 10, 13, 15, 20, 21 and 25,We observe a rotational effect of the parameters$\varepsilon, \lambda_1, \mathbb{F}_3, t, U, Gr$and Reindicating a decrease in velocity with an increase in$\varepsilon, \lambda_1, \mathbb{F}_3, t, U, Gr$and Re in the region $r < 0.2$ and increase in velocity with an increase in$\varepsilon, \lambda_1, \mathbb{F}_3, t, U, Gr$and Re in the

region$r > 0.2$.Figures 19 and 23 illustrate the behavior of velocity (w) with variations in ζ and Pr. It is observed that there is a decrease in velocity with an increase in Ω and Rn. Figures 22 and 24 depict the behavior of velocity (w) with variations in Ω and Rn. It is observed that there is an increase in velocity with an increase in Ω and Rn.

5.3 Trapping Phenomena

The creation of a fluid bolus through enclosed streamlines, leading to internal circulation, is referred to as trapping. This confined bolus is subsequently propelled forward in conjunction with the peristaltic wave. In accordance with equation 35, the parameters effects $\varepsilon, \emptyset, \lambda_1, \mathbb{F}_5, \mathbb{F}_4, \mathbb{F}_3, \mathbb{F}_1, t, \mathbb{F}_2, Da, \alpha, \zeta, U, Gr, \Omega, Pr, Rn, Re, Fr, \varrho$and$\Sigma$on trapping is visually evident in figures 29-45.Figures 29, 31, 34, 36, 41, and 43 indicate a gradual reduction in the volume of the trapped bolus with increasing values of ε, λ_1, F_3, t, U, and Re, particularly in the middle of the channel. This trend leads to the transformation of the peristaltic wave into a bolus.Figures 30, 32, 33, 35, 37, 38, 39, 40, 44, and 45 reveal an enlargement in the size of the trapped bolus positioned at the center of the channel with increasing values of Ø, $\mathbb{F}_5$, $\mathbb{F}_4$, $\mathbb{F}_1$, $\mathbb{F}_2$, Da, α, Fr, ϱ, and Σ. This leads to a transformation of the bolus into a wave. Additionally, it is noteworthy that the parameters Gr, Ω, Pr, Rn, and ϱ exhibit relatively weak effects.

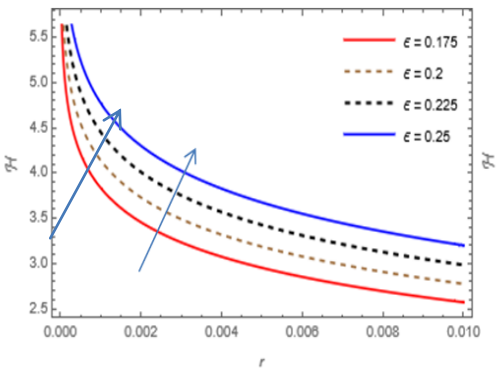

Figure 2: Changes in temperature$\mathbb{H}$ vs. r at $Rn = 0.1, Pr = 2, \Omega = 0.9, \emptyset = 0.2, z = 0.1t = 0.05,$

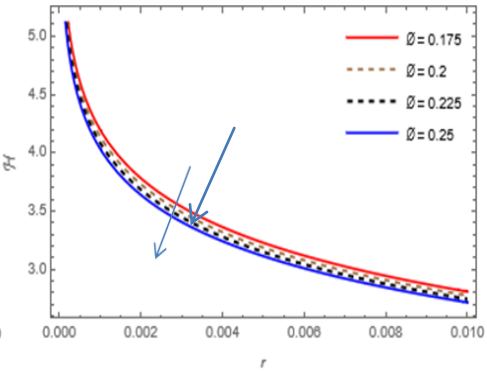

Figure 3: Changes in temperature$\mathbb{H}$ vs. r at $Rn = 0.1, Pr = 2, \Omega = 0.9, \epsilon = 0.2, z = 0.1t = 0.05,$

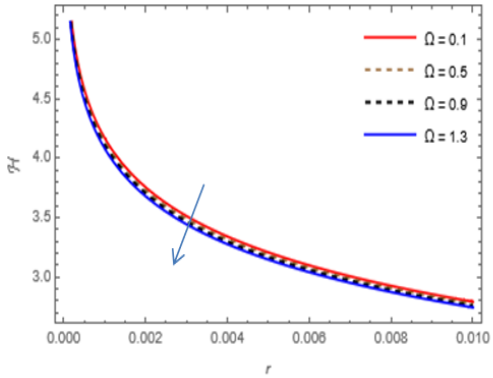

Figure 4: Temperature variations $\mathbb{H}$ vs. r at $Rn = 0.1, Pr = 2, \emptyset = 0.2, \epsilon = 0.2, z = 0.1t = 0.05,$

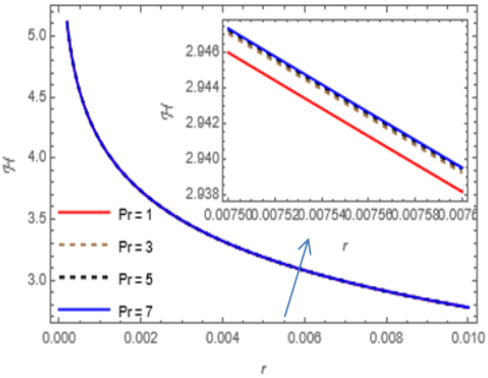

Figure 5: Changes in temperature$\mathbb{H}$ vs. r at $Rn = 0.1, \Omega = 0.9, \emptyset = 0.2, \epsilon = 0.2, z = 0.1t = 0.05,$

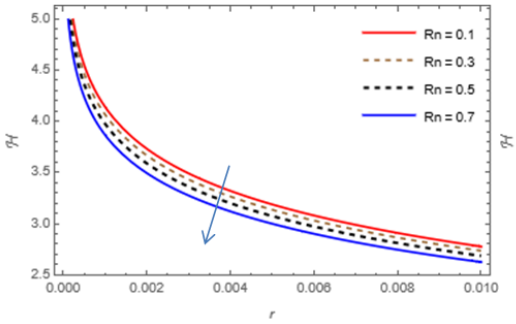

Figure 6: Changes in temperature$\mathbb{H}$ vs. r at $Pr = 2, \Omega = 0.9, \emptyset = 0.2, \epsilon = 0.2, z = 0.1 t = 0.05,$

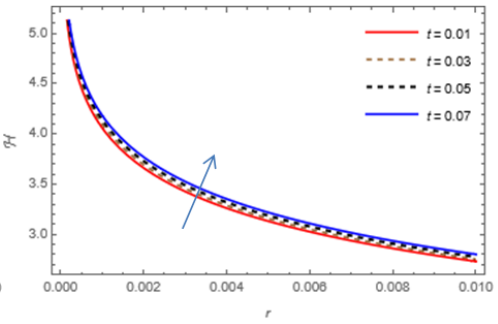

Figure 7: Changes in temperature$\mathbb{H}$ vs. r at $Pr = 2, \Omega = 0.9, \emptyset = 0.2, \epsilon = 0.2, z = 0.1 Rn = 0.1,$

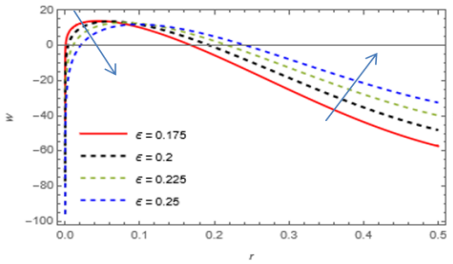

Figure 8: Distribution of velocity for different values of$\varepsilon$with$\lambda_1 = 0.1, \emptyset = 0.2, \mathbb{F}_5 = 0.1, \mathbb{F}_3 = 0.1, \mathbb{F}_4 = 0.5, \mathbb{F}_1 = 0.1, t = 0.05, \mathbb{F}_2 = 0.5, Da = 0.9, \alpha = 3.75, \zeta = 0.5, U = 1.1, Gr = 2, \Omega = 0.9, Pr = 2, Rn = 0.1, Re = 1, Fr = 0.5, \varrho = \frac{\pi}{3}, \Sigma = \frac{\pi}{4}, z = 0.1.$

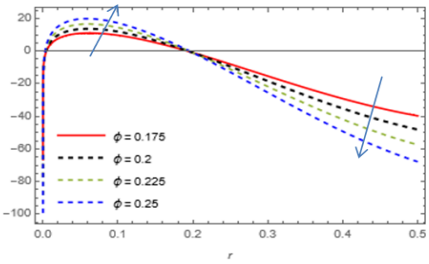

Figure 9: Distribution of velocity for different value of $\emptyset$with $\varepsilon = 0.2, \lambda_1 = 0.1, \mathbb{F}_5 = 0.1, \mathbb{F}_3 = 0.1, \mathbb{F}_4 = 0.5, \mathbb{F}_1 = 0.1, t = 0.05, \mathbb{F}_2 = 0.5, Da = 0.9, \alpha = 3.75, \zeta = 0.5, U = 1.1, Gr = 2, \Omega = 0.9, Pr = 2, Rn = 0.1, Re = 1, Fr = 0.5, \varrho = \frac{\pi}{3}, \Sigma = \frac{\pi}{4}, z = 0.1.$

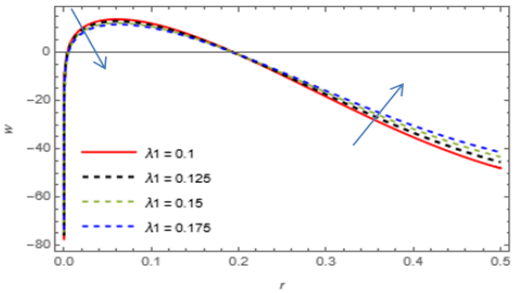

Figure 10: Spread of Velocity for different values of$\lambda_1$with $\varepsilon = 0.2, \emptyset = 0.2, \mathbb{F}_5 = 0.1, \mathbb{F}_4 = 0.5, \mathbb{F}_3 = 0.1, \mathbb{F}_1 = 0.1, t = 0.05, \mathbb{F}_2 = 0.5, Da = 0.9, \alpha = 3.75, \zeta = 0.5, U = 1.1, Gr = 2, \Omega = 0.9, Pr = 2, Rn = 0.1, Re = 1, Fr = 0.5, \varrho = \frac{\pi}{3}, \Sigma = \frac{\pi}{4}, z = 0.1.$

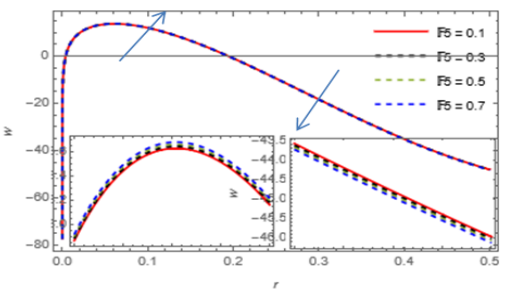

Figure 11: Spread of velocity for different values of$\mathbb{F}_5$with $\varepsilon = 0.2, \emptyset = 0.2, \lambda_1 = 0.1, \mathbb{F}_4 = 0.5, \mathbb{F}_1 = 0.1, \mathbb{F}_3 = 0.1, t = 0.05, \mathbb{F}_2 = 0.5, Da = 0.9, \alpha = 3.75, \zeta = 0.5, U = 1.1, Gr = 2, \Omega = 0.9, Pr = 2, Rn = 0.1, Re = 1, Fr = 0.5, \varrho = \frac{\pi}{3}, \Sigma = \frac{\pi}{4}, z = 0.1.$

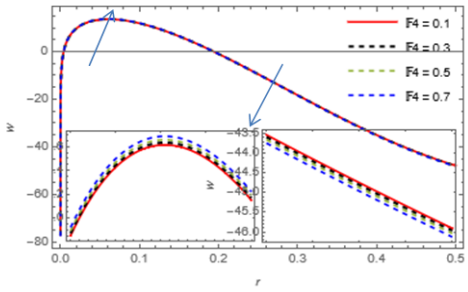

Figure 12: Spread of velocity for different values of $\mathbb{F}_4$ with $\varepsilon = 0.2, \emptyset = 0.2, \lambda_1 = 0.1, \mathbb{F}_5 = 0.1, \mathbb{F}_1 = 0.1, \mathbb{F}_3 = 0.1, t = 0.05, \mathbb{F}_2 = 0.5, Da = 0.9, \alpha = 3.75, \zeta = 0.5, U = 1.1, Gr = 2, \Omega = 0.9, Pr = 2, Rn = 0.1, Re = 1, Fr = 0.5, \varrho = \frac{\pi}{3}, \Sigma = \frac{\pi}{4}, z = 0.1$.

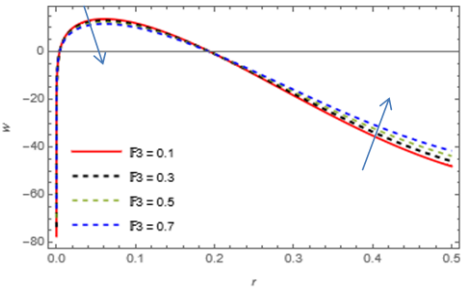

Figure 13: Spread of velocity for differen values of $\mathbb{F}_3$ with $\varepsilon = 0.2, \emptyset = 0.2, \lambda_1 = 0.1, \mathbb{F}_5 = 0.1, \mathbb{F}_4 = 0.5, \mathbb{F}_1 = 0.1, t = 0.05, \mathbb{F}_2 = 0.5, Da = 0.9, \alpha = 3.75, \zeta = 0.5, U = 1.1, Gr = 2, \Omega = 0.9, Pr = 2, Rn = 0.1, Re = 1, Fr = 0.5, \varrho = \frac{\pi}{3}, \Sigma = \frac{\pi}{4}, z = 0.1$.

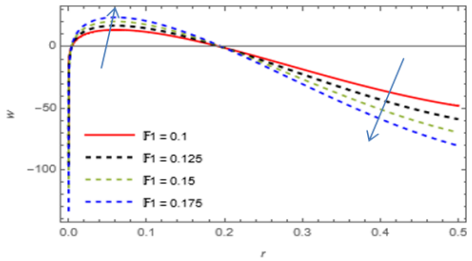

Figure 14: Spread of velocity for different values of $\mathbb{F}_1$ with $\varepsilon = 0.2, \emptyset = 0.2, \lambda_1 = 0.1, \mathbb{F}_5 = 0.1, \mathbb{F}_4 = 0.5, \mathbb{F}_3 = 0.1, t = 0.05, \mathbb{F}_2 = 0.5, Da = 0.9, \alpha = 3.75, \zeta = 0.5, U = 1.1, Gr = 2, \Omega = 0.9, Pr = 2, Rn = 0.1, Re = 1, Fr = 0.5, \varrho = \frac{\pi}{3}, \Sigma = \frac{\pi}{4}, z = 0.1$.

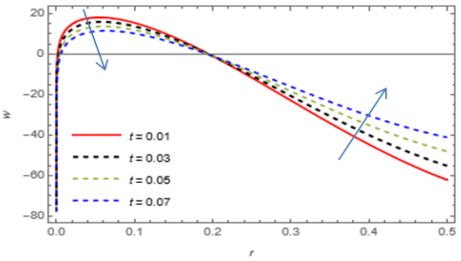

Figure 15: Spread of velocity for differen values of t with $\varepsilon = 0.2, \emptyset = 0.2, \lambda_1 = 0.1, \mathbb{F}_5 = 0.1, \mathbb{F}_4 = 0.5, \mathbb{F}_1 = 0.1, \mathbb{F}_3 = 0.1, \mathbb{F}_2 = 0.5, Da = 0.9, \alpha = 3.75, \zeta = 0.5, U = 1.1, Gr = 2, \Omega = 0.9, Pr = 2, Rn = 0.1, Re = 1, Fr = 0.5, \varrho = \frac{\pi}{3}, \Sigma = \frac{\pi}{4}, z = 0.1$.

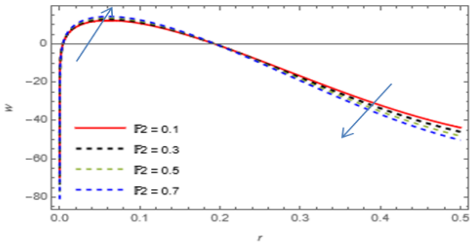

Figure 16: Velocity division for different values of $\mathbb{F}_2$ with $\varepsilon = 0.2, \emptyset = 0.2, \lambda_1 = 0.1, \mathbb{F}_5 = 0.1, \mathbb{F}_4 = 0.5, \mathbb{F}_1 = 0.1, \mathbb{F}_3 = 0.1, t = 0.05, Da = 0.9, \alpha = 3.75, \zeta = 0.5, U = 1.1, Gr = 2, \Omega = 0.9, Pr = 2, Rn = 0.1, Re = 1, Fr = 0.5, \varrho = \frac{\pi}{3}, \Sigma = \frac{\pi}{4}, z = 0.1$.

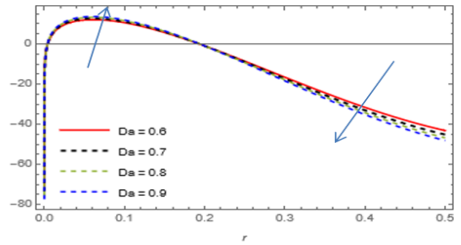

Figure 17: Velocity division for different values of Da with $\varepsilon = 0.2, \emptyset = 0.2, \lambda_1 = 0.1, \mathbb{F}_5 = 0.1, \mathbb{F}_4 = 0.5, \mathbb{F}_1 = 0.1, \mathbb{F}_3 = 0.1, t = 0.05, \mathbb{F}_2 = 0.5, \alpha = 3.75, \zeta = 0.5, U = 1.1, Gr = 2, \Omega = 0.9, Pr = 2, Rn = 0.1, Re = 1, Fr = 0.5, \varrho = \frac{\pi}{3}, \Sigma = \frac{\pi}{4}, z = 0.1$.

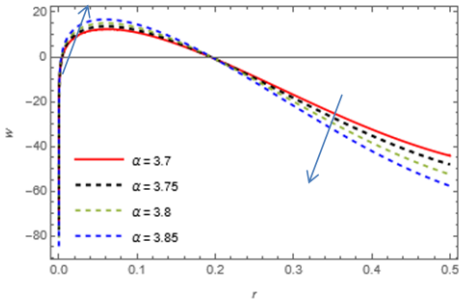

Figure 18: Velocity divisionfor different values of$\alpha$with $\varepsilon = 0.2, \emptyset = 0.2, \lambda_1 = 0.1, \mathbb{F}_5 = 0.1, \mathbb{F}_4 = 0.5, \mathbb{F}_1 = 0.1, \mathbb{F}_3 = 0.1, t = 0.05, \mathbb{F}_2 = 0.5, Da = 0.9, \zeta = 0.5, U = 1.1, Gr = 2, \Omega = 0.9, Pr = 2, Rn = 0.1, Re = 1, Fr = 0.5, \varrho = \frac{\pi}{3}, \Sigma = \frac{\pi}{4}, z = 0.1.$

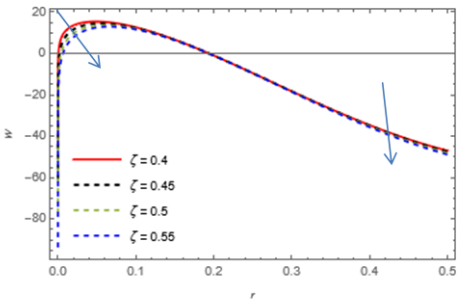

Figure 19: Velocitydivisionfor differen values of$\zeta$with $\varepsilon = 0.2, \emptyset = 0.2, \lambda_1 = 0.1, \mathbb{F}_5 = 0.1, \mathbb{F}_4 = 0.5, \mathbb{F}_1 = 0.1, \mathbb{F}_3 = 0.1, t = 0.05, \mathbb{F}_2 = 0.5, Da = 0.9, \alpha = 3.75, U = 1.1, Gr = 2, \Omega = 0.9, Pr = 2, Rn = 0.1, Re = 1, Fr = 0.5, \varrho = \frac{\pi}{3}, \Sigma = \frac{\pi}{4}, z = 0.1.$

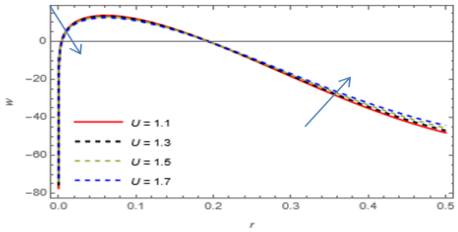

Figure 20: division of velocity for different values of$U$with $\varepsilon = 0.2, \emptyset = 0.2, \lambda_1 = 0.1, \mathbb{F}_5 = 0.1, \mathbb{F}_4 = 0.5, \mathbb{F}_1 = 0.1, \mathbb{F}_3 = 0.1, t = 0.05, \mathbb{F}_2 = 0.5, Da = 0.9, \alpha = 3.75, \zeta = 0.5, Gr = 2, \Omega = 0.9, Pr = 2, Rn = 0.1, Re = 1, Fr = 0.5, \varrho = \frac{\pi}{3}, \Sigma = \frac{\pi}{4}, z = 0.1.$

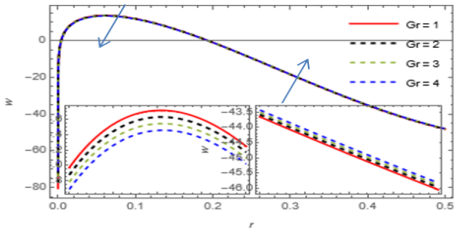

Figure 21: division of velocity for different values of$Gr$with $\varepsilon = 0.2, \emptyset = 0.2, \lambda_1 = 0.1, \mathbb{F}_5 = 0.1, \mathbb{F}_4 = 0.5, \mathbb{F}_1 = 0.1, \mathbb{F}_3 = 0.1, t = 0.05, \mathbb{F}_2 = 0.5, Da = 0.9, \alpha = 3.75, \zeta = 0.5, U = 1.1, \Omega = 0.9, Pr = 2, Rn = 0.1, Re = 1, Fr = 0.5, \varrho = \frac{\pi}{3}, \Sigma = \frac{\pi}{4}, z = 0.1.$

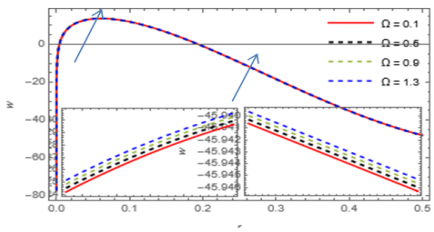

Figure 22: division of velocity for different values of$\Omega$with $\varepsilon = 0.2, \emptyset = 0.2, \lambda_1 = 0.1, \mathbb{F}_5 = 0.1, \mathbb{F}_4 = 0.5, \mathbb{F}_1 = 0.1, \mathbb{F}_3 = 0.1, t = 0.05, \mathbb{F}_2 = 0.5, Da = 0.9, \alpha = 3.75, \zeta = 0.5, U = 1.1, Gr = 2, Pr = 2, Rn = 0.1, Re = 1, Fr = 0.5, \varrho = \frac{\pi}{3}, \Sigma = \frac{\pi}{4}, z = 0.1.$

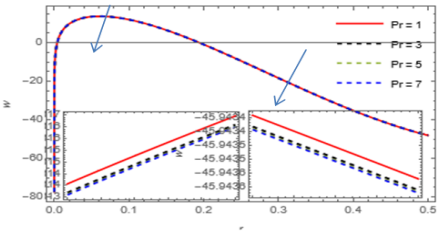

Figure 23: division of velocity for differen values of$Pr$with $\varepsilon = 0.2, \emptyset = 0.2, \lambda_1 = 0.1, \mathbb{F}_5 = 0.1, \mathbb{F}_4 = 0.5, \mathbb{F}_1 = 0.1, \mathbb{F}_3 = 0.1, t = 0.05, \mathbb{F}_2 = 0.5, Da = 0.9, \alpha = 3.75, \zeta = 0.5, U = 1.1, Gr = 2, \Omega = 0.9, Rn = 0.1, Re = 1, Fr = 0.5, \varrho = \frac{\pi}{3}, \Sigma = \frac{\pi}{4}, z = 0.1.$

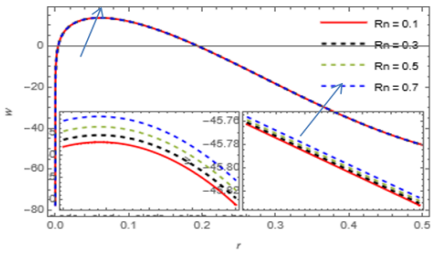

Figure 24: velocitydivision fordifferent values of $Rn$with $\varepsilon = 0.2, \emptyset = 0.2, \lambda_1 = 0.1, \mathbb{F}_5 = 0.1, \mathbb{F}_4 = 0.5, \mathbb{F}_1 = 0.1, \mathbb{F}_3 = 0.1, t = 0.05, \mathbb{F}_2 = 0.5, Da = 0.9, \alpha = 3.75, \zeta = 0.5, U = 1.1, Gr = 2, \Omega = 0.9, Pr = 2, Re = 1, Fr = 0.5, \varrho = \frac{\pi}{3}, \Sigma = \frac{\pi}{4}, z = 0.1.$

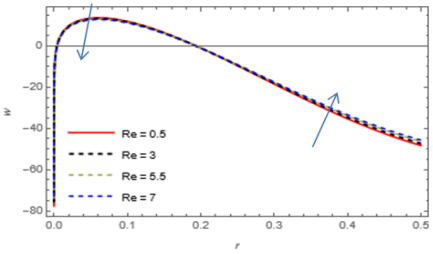

Figure 25: velocitydivisionfor different values of $Re$with $\varepsilon = 0.2, \emptyset = 0.2, \lambda_1 = 0.1, \mathbb{F}_5 = 0.1, \mathbb{F}_4 = 0.5, \mathbb{F}_1 = 0.1, \mathbb{F}_3 = 0.1, t = 0.05, \mathbb{F}_2 = 0.5, Da = 0.9, \alpha = 3.75, \zeta = 0.5, U = 1.1, Gr = 2, \Omega = 0.9, Pr = 2, Rn = 0.1, Fr = 0.5, \varrho = \frac{\pi}{3}, \Sigma = \frac{\pi}{4}, z = 0.1.$

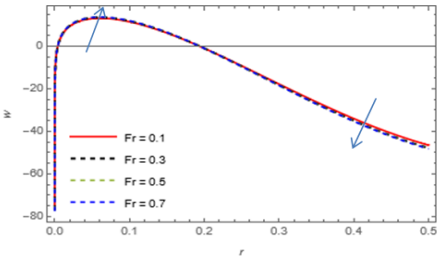

Figure 26:division of velocity for different values of$Fr$with $\varepsilon = 0.2, \emptyset = 0.2, \lambda_1 = 0.1, \mathbb{F}_5 = 0.1, \mathbb{F}_4 = 0.5, \mathbb{F}_1 = 0.1, \mathbb{F}_3 = 0.1, t = 0.05, \mathbb{F}_2 = 0.5, Da = 0.9, \alpha = 3.75, \zeta = 0.5, U = 1.1, Gr = 2, \Omega = 0.9, Pr = 2, Rn = 0.1, Re = 1, \varrho = \frac{\pi}{3}, \Sigma = \frac{\pi}{4}, z = 0.1.$

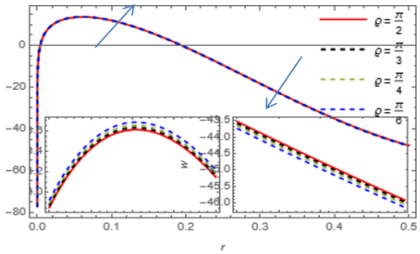

Figure 27:division of velocity for different values of$\varrho$with $\varepsilon = 0.2, \emptyset = 0.2, \lambda_1 = 0.1, \mathbb{F}_5 = 0.1, \mathbb{F}_4 = 0.5, \mathbb{F}_1 = 0.1, \mathbb{F}_3 = 0.1, t = 0.05, \mathbb{F}_2 = 0.5, Da = 0.9, \alpha = 3.75, \zeta = 0.5, U = 1.1, Gr = 2, \Omega = 0.9, Pr = 2, Rn = 0.1, Re = 1, Fr = 0.5, \Sigma = \frac{\pi}{4}, z = 0.1.$

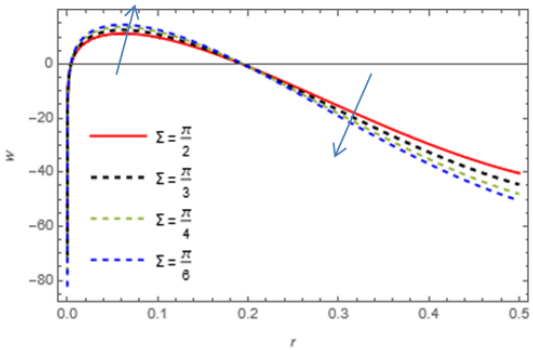

Figure 28:division of velocity for different values of$\Sigma$with $\varepsilon = 0.2, \emptyset = 0.2, \lambda_1 = 0.1, \mathbb{F}_5 = 0.1, \mathbb{F}_4 = 0.5, \mathbb{F}_1 = 0.1, \mathbb{F}_3 = 0.1, t = 0.05, \mathbb{F}_2 = 0.5, Da = 0.9, \alpha = 3.75, \zeta = 0.5, U = 1.1, Gr = 2, \Omega = 0.9, Pr = 2, Rn = 0.1, Re = 1, Fr = 0.5, \varrho = \frac{\pi}{3}, z = 0.1.$

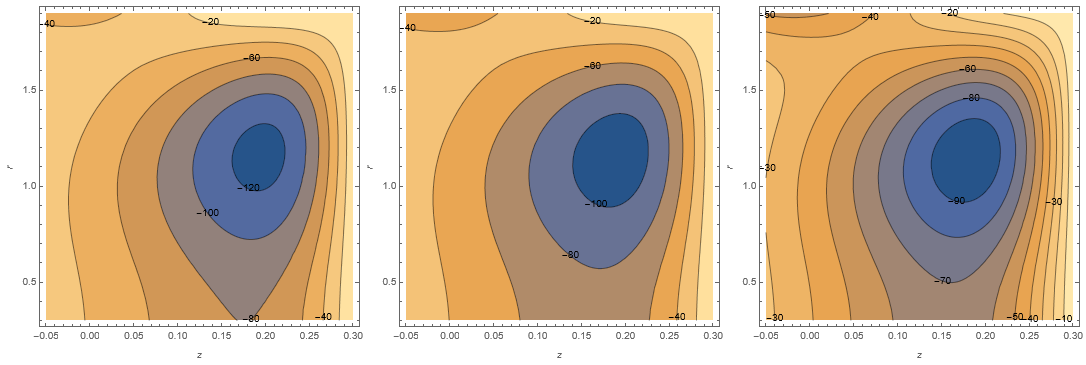

Figure 29: The wave frame for varying ε values, $\varepsilon = \{0.175,0.2,0.225\}$ at$\phi = 0.2, \lambda_1 = 0.1, \mathbb{F}_5 = 0.1, \mathbb{F}_4 = 0.5, \mathbb{F}_1 = 0.1, \mathbb{F}_3 = 0.1, t = 0.05, \mathbb{F}_2 = 0.5, Da = 0.9, \alpha = 3.75, \zeta = 0.5, U = 1.1, Gr = 2, \Omega = 0.9, Pr = 2, Rn = 0.1, Re = 0.1, Fr = 0.5, \varrho = \frac{\pi}{3}, \Sigma = \frac{\pi}{4}$.

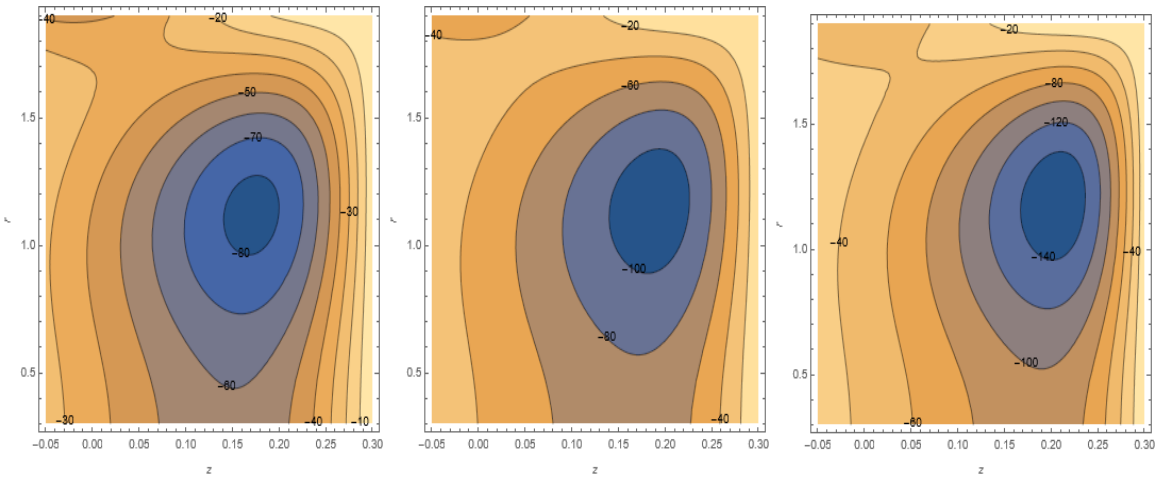

Figure 30: The wave frame for varying ϕ values, $\phi = \{0.175,0.2,0.225\}at\varepsilon = 0.2, \lambda_1 = 0.1, \mathbb{F}_5 = 0.1, \mathbb{F}_4 = 0.5, \mathbb{F}_1 = 0.1, \mathbb{F}_3 = 0.1, t = 0.05, \mathbb{F}_2 = 0.5, Da = 0.9, \alpha = 3.75, \zeta = 0.5, U = 1.1, Gr = 2, \Omega = 0.9, Pr = 2, Rn = 0.1, Re = 0.1, Fr = 0.5, \varrho = \frac{\pi}{3}, \Sigma = \frac{\pi}{4}$.

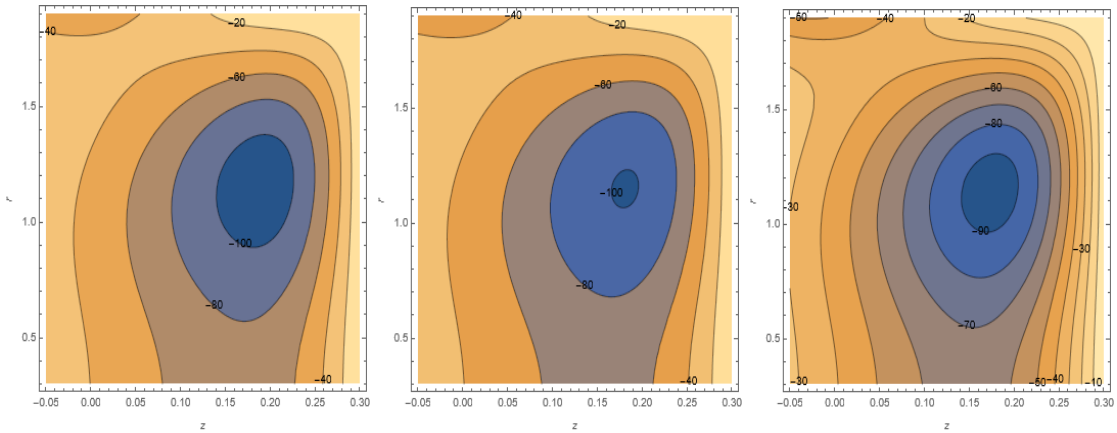

Figure 31: The wave frame for varying λ_1 values, $\lambda_1 = \{0.1,0.125,0.15\}at\varepsilon = 0.2, \phi = 0.2, \mathbb{F}_5 = 0.1, \mathbb{F}_4 = 0.5, \mathbb{F}_1 = 0.1, \mathbb{F}_3 = 0.1, t = 0.05, \mathbb{F}_2 = 0.5, Da = 0.9, \alpha = 3.75, \zeta = 0.5, U = 1.1, Gr = 2, \Omega = 0.9, Pr = 2, Rn = 0.1, Re = 0.1, Fr = 0.5, \varrho = \frac{\pi}{3}, \Sigma = \frac{\pi}{4}$.

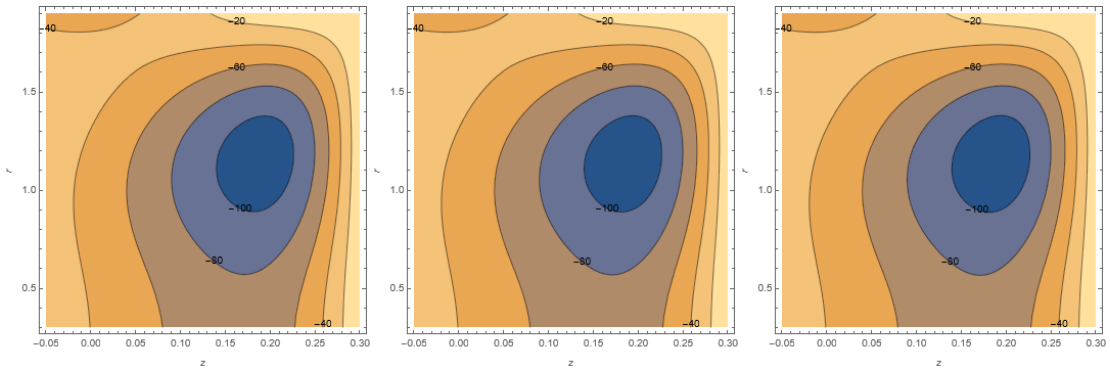

Figure 32: The wave frame for varying $\mathbb{F}_5$ values,$\mathbb{F}_5 = \{0.1,0.3,0.5\}at\varepsilon = 0.2, \phi = 0.2, \lambda_1 = 0.1, \mathbb{F}_4 = 0.5, \mathbb{F}_1 = 0.1, \mathbb{F}_3 = 0.1, t = 0.05, \mathbb{F}_2 = 0.5, Da = 0.9, \alpha = 3.75, \zeta = 0.5, U = 1.1, Gr = 2, \Omega = 0.9, Pr = 2, Rn = 0.1, Re = 0.1, Fr = 0.5, \varrho = \frac{\pi}{3}, \Sigma = \frac{\pi}{4}$.

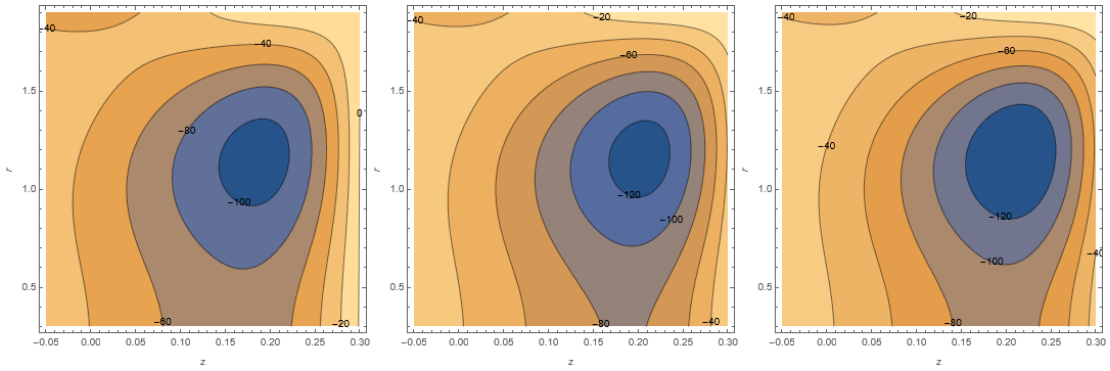

Figure 33: The wave frame for varying $\mathbb{F}_4$values, $\mathbb{F}_4 = \{0.1,0.3,0.5\}at\varepsilon = 0.2, \phi = 0.2, \lambda_1 = 0.1, \mathbb{F}_5 = 0.1, \mathbb{F}_3 = 0.1, \mathbb{F}_1 = 0.1, t = 0.05, \mathbb{F}_2 = 0.5, Da = 0.9, \alpha = 3.75, \zeta = 0.5, U = 1.1, Gr = 2, \Omega = 0.9, Pr = 2, Rn = 0.1, Re = 0.1, Fr = 0.5, \varrho = \frac{\pi}{3}, \Sigma = \frac{\pi}{4}$.

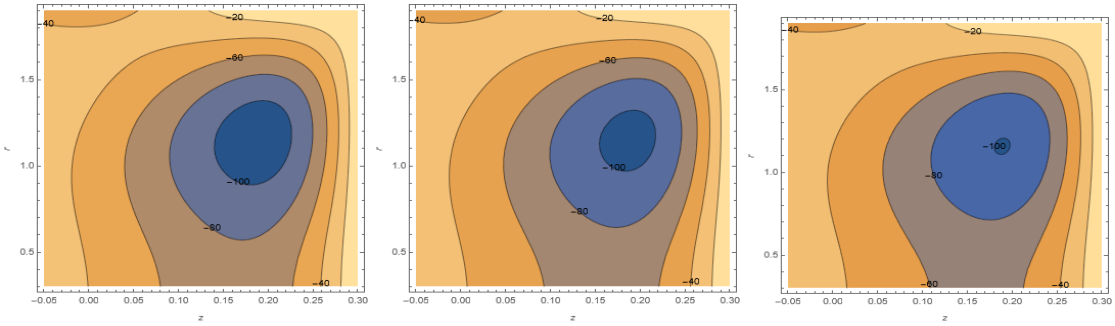

Figure 34: The wave framefor varying $\mathbb{F}_3$ values,$\mathbb{F}_3 = \{0.1,0.3,0.5\}at\varepsilon = 0.2, \phi = 0.2, \lambda_1 = 0.1, \mathbb{F}_5 = 0.1, \mathbb{F}_4 = 0.5, \mathbb{F}_1 = 0.1, t = 0.05, \mathbb{F}_2 = 0.5, Da = 0.9, \alpha = 3.75, \zeta = 0.5, U = 1.1, Gr = 2, \Omega = 0.9, Pr = 2, Rn = 0.1, Re = 0.1, Fr = 0.5, \varrho = \frac{\pi}{3}, \Sigma = \frac{\pi}{4}$.

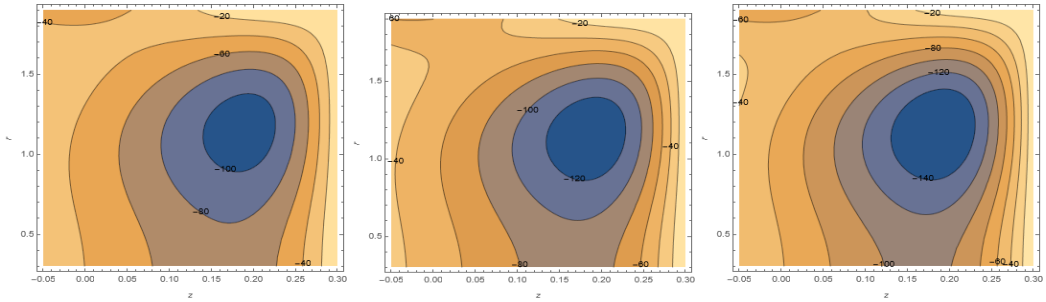

Figure 35: The wave framefor varying $\mathbb{F}_1$ values, $\mathbb{F}_1 = \{0.1,0.125,0.15\}at\varepsilon = 0.2, \phi = 0.2, \lambda_1 = 0.1, \mathbb{F}_5 = 0.1, \mathbb{F}_4 = 0.5, \mathbb{F}_3 = 0.1, t = 0.05, \mathbb{F}_2 = 0.5, Da = 0.9, \alpha = 3.75, \zeta = 0.5, U = 1.1, Gr = 2, \Omega = 0.9, Pr = 2, Rn = 0.1, Re = 0.1, Fr = 0.5, \varrho = \frac{\pi}{3}, \Sigma = \frac{\pi}{4}$.

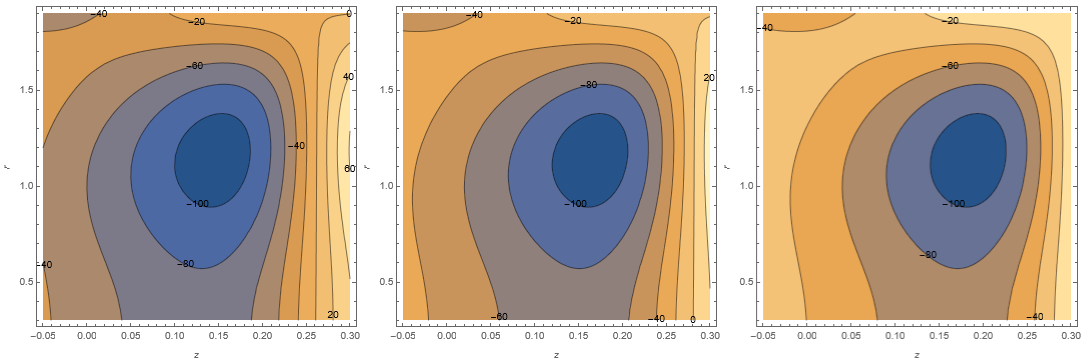

Figure 36: The wave frame for varying t values,$t = \{0.01,0.03,0.05\}$at$\varepsilon = 0.2, \phi = 0.2, \lambda_1 = 0.1, \mathbb{F}_5 = 0.1, \mathbb{F}_4 = 0.5, \mathbb{F}_1 = 0.1, \mathbb{F}_3 = 0.1, \mathbb{F}_2 = 0.5, Da = 0.9, \alpha = 3.75, \zeta = 0.5, U = 1.1, Gr = 2, \Omega = 0.9, Pr = 2, Rn = 0.1, Re = 0.1, Fr = 0.5, \varrho = \frac{\pi}{3}, \Sigma = \frac{\pi}{4}$.

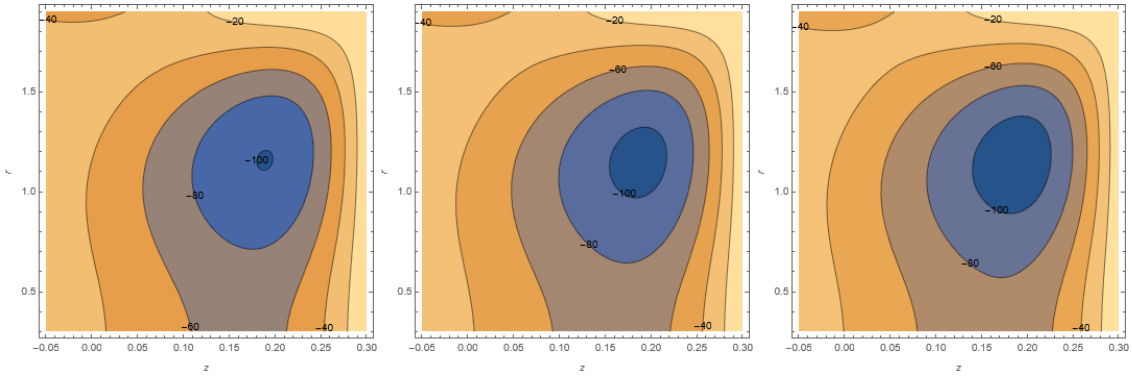

Figure 37: The wave framefor varying $\mathbb{F}_2$ values, $\mathbb{F}_2 = \{0.1,0.3,0.5\}at\varepsilon = 0.2, \phi = 0.2, \lambda_1 = 0.1, \mathbb{F}_5 = 0.1, \mathbb{F}_4 = 0.5, \mathbb{F}_1 = 0.1, \mathbb{F}_3 = 0.1, t = 0.05, Da = 0.9, \alpha = 3.75, \zeta = 0.5, U = 1.1, Gr = 2, \Omega = 0.9, Pr = 2, Rn = 0.1, Re = 0.1, Fr = 0.5, \varrho = \frac{\pi}{3}, \Sigma = \frac{\pi}{4}$.

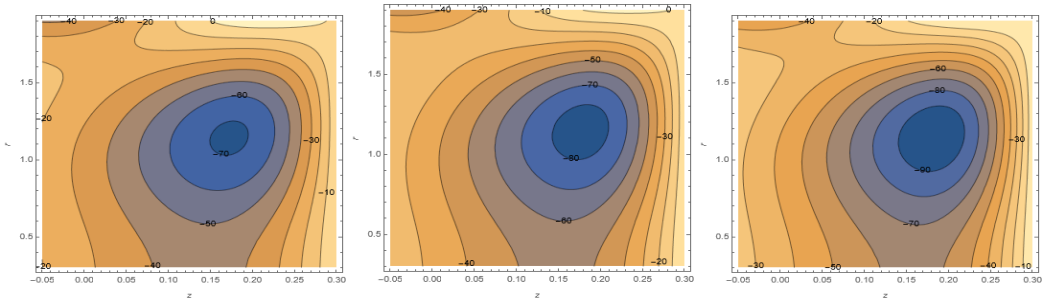

Figure 38: The wave framefor varying Da values, $Da = \{0.6,0.7,0.8\}$at$\varepsilon = 0.2, \phi = 0.2, \lambda_1 = 0.1, \mathbb{F}_5 = 0.1, \mathbb{F}_4 = 0.5, \mathbb{F}_1 = 0.1, \mathbb{F}_3 = 0.1, t = 0.05, \mathbb{F}_2 = 0.5, \alpha = 3.75, \zeta = 0.5, U = 1.1, Gr = 2, \Omega = 0.9, Pr = 2, Rn = 0.1, Re = 0.1, Fr = 0.5, \varrho = \frac{\pi}{3}, \Sigma = \frac{\pi}{4}$.

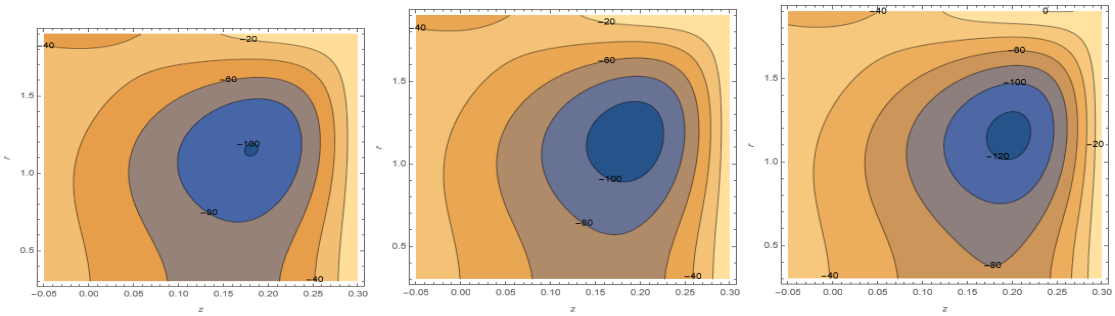

Figure 39: The wave framefor varying α values,$\alpha = \{3.7,3.75,3.8\}at\varepsilon = 0.2, \phi = 0.2, \lambda_1 = 0.1, \mathbb{F}_5 = 0.1, \mathbb{F}_4 = 0.5, \mathbb{F}_1 = 0.1, \mathbb{F}_3 = 0.1, \mathrm{t} = 0.05, \mathbb{F}_2 = 0.5, \mathrm{Da} = 0.9, \zeta = 0.5, \mathrm{U} = 1.1, \mathrm{Gr} = 2, \Omega = 0.9, \mathrm{Pr} = 2, \mathrm{Rn} = 0.1, \mathrm{Re} = 0.1, \mathrm{Fr} = 0.5, \varrho = \frac{\pi}{3}, \Sigma = \frac{\pi}{4}$.

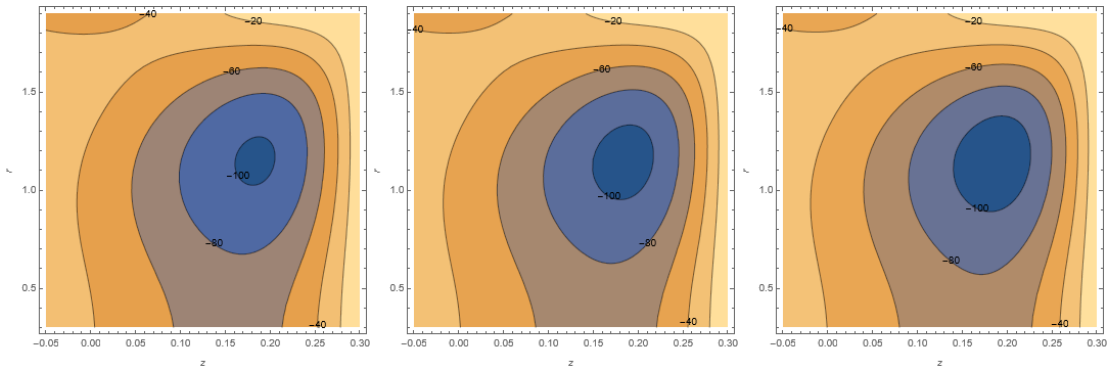

Figure 40: The wave framefor varying ζ values,$\zeta = \{0.4,0.45,0.5\}$at$\varepsilon = 0.2, \phi = 0.2, \lambda_1 = 0.1, \mathbb{F}_5 = 0.1, \mathbb{F}_4 = 0.5, \mathbb{F}_1 = 0.1, \mathbb{F}_3 = 0.1, t = 0.05, \mathbb{F}_2 = 0.5, Da = 0.9, \alpha = 3.75, U = 1.1, Gr = 2, \Omega = 0.9, Pr = 2, Rn = 0.1, Re = 0.1, Fr = 0.5, \varrho = \frac{\pi}{3}, \Sigma = \frac{\pi}{4}$.

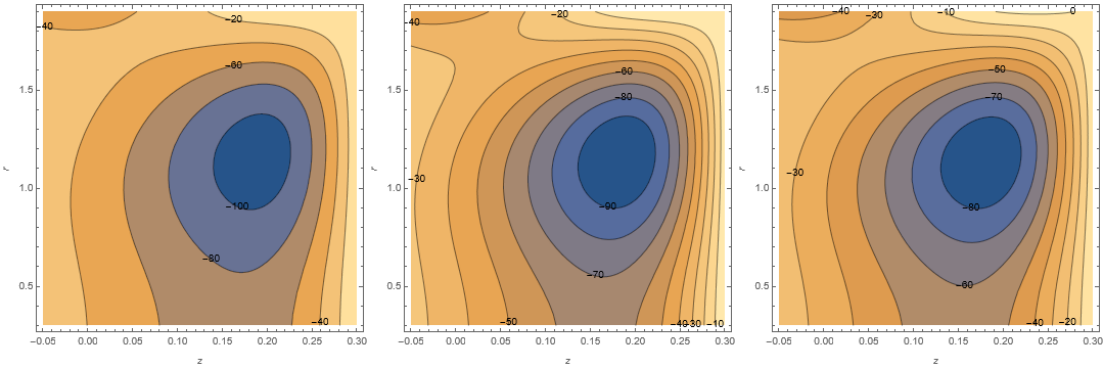

Figure 41: The wave framefor varying U values, $U = \{1.1,1.3,1.5\}$at$\varepsilon = 0.2, \phi = 0.2, \lambda_1 = 0.1, \mathbb{F}_5 = 0.1, \mathbb{F}_4 = 0.5, \mathbb{F}_1 = 0.1, \mathbb{F}_3 = 0.1, t = 0.05, \mathbb{F}_2 = 0.5, Da = 0.9, \alpha = 3.75, \zeta = 0.5, Gr = 2, \Omega = 0.9, Pr = 2, Rn = 0.1, Re = 0.1, Fr = 0.5, \varrho = \frac{\pi}{3}, \Sigma = \frac{\pi}{4}$.

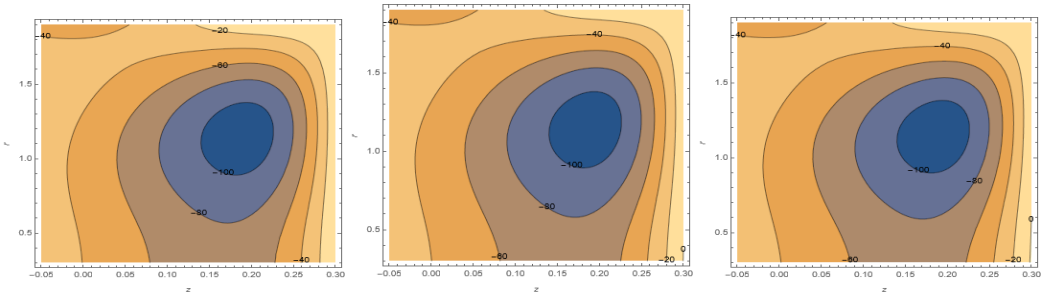

Figure 42: The wave framefor varying Gr values, $Gr = \{0.1,0.5,0.9\}$at$\varepsilon = 0.2, \phi = 0.2, \lambda_1 = 0.1, \mathbb{F}_5 = 0.1, \mathbb{F}_4 = 0.5, \mathbb{F}_1 = 0.1, \mathbb{F}_3 = 0.1, t = 0.05, \mathbb{F}_2 = 0.5, Da = 0.9, \alpha = 3.75, \zeta = 0.5, U = 1.1, \Omega = 0.9, Pr = 2, Rn = 0.1, Re = 0.1, Fr = 0.5, \varrho = \frac{\pi}{3}, \Sigma = \frac{\pi}{4}$.

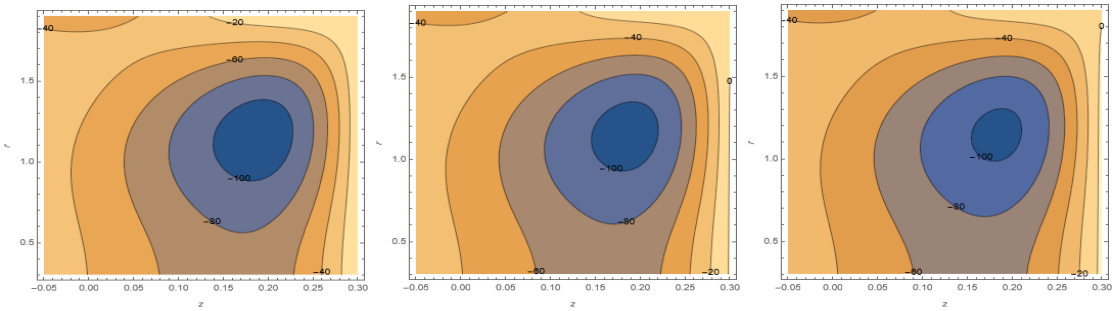

Figure 43: The wave framefor varying Re values, $Re = \{0.5,3,5.5\}$at$\varepsilon = 0.2, \phi = 0.2, \lambda_1 = 0.1, \mathbb{F}_5 = 0.1, \mathbb{F}_4 = 0.5, \mathbb{F}_1 = 0.1, \mathbb{F}_3 = 0.1, t = 0.05, \mathbb{F}_2 = 0.5, Da = 0.9, \alpha = 3.75, \zeta = 0.5, U = 1.1, Gr = 2, \Omega = 0.9, Pr = 2, Rn = 0.1, Fr = 0.5, \varrho = \frac{\pi}{3}, \Sigma = \frac{\pi}{4}$.

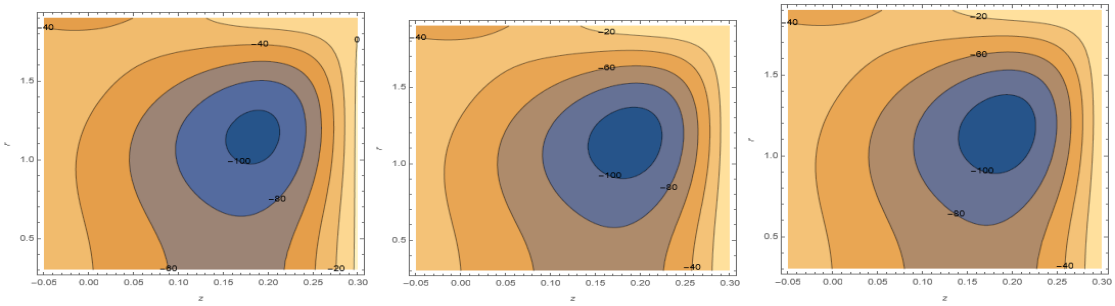

Figure 44: The wave framefor varying Fr values, $Fr = \{0.1,0.3,0.5\}$at$\varepsilon = 0.2, \phi = 0.2, \lambda_1 = 0.1, \mathbb{F}_5 = 0.1, \mathbb{F}_4 = 0.5, \mathbb{F}_1 = 0.1, \mathbb{F}_3 = 0.1, t = 0.05, \mathbb{F}_2 = 0.5, Da = 0.9, \alpha = 3.75, \zeta = 0.5, U = 1.1, Gr = 2, \Omega = 0.9, Pr = 2, Rn = 0.1, Re = 0.1, \varrho = \frac{\pi}{3}, \Sigma = \frac{\pi}{4}$.

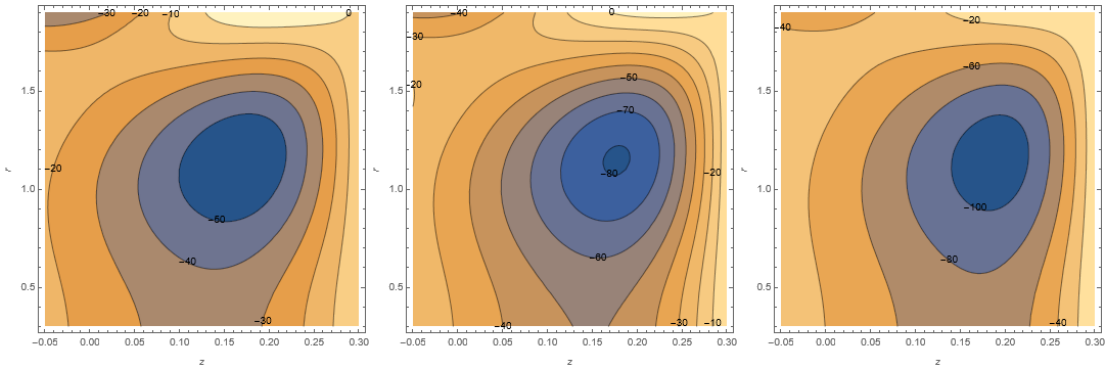

Figure 45: The wave framefor varying Σ values, $\Sigma = \left\{\frac{\pi}{2}, \frac{\pi}{3}, \frac{\pi}{4}\right\}at\varepsilon = 0.2, \phi = 0.2, \lambda_1 = 0.1, \mathbb{F}_5 = 0.1, \mathbb{F}_4 = 0.5, \mathbb{F}_1 = 0.1, \mathbb{F}_3 = 0.1, t = 0.05, \mathbb{F}_2 = 0.5, Da = 0.9, \alpha = 3.75, \zeta = 0.5, U = 1.1, Gr = 2, \Omega = 0.9, Pr = 2, Rn = 0.1, Re = 0.1, Fr = 0.5, \varrho = \frac{\pi}{3}$.

REFERENCES

[1] Latham TW. Fluid motions in a peristaltic pump, S.M. Thesis, MIT, 1966.

[2] M. Kothandapani, S. Srinivas" On the influence of wall properties in the MHD peristaltic transport with heat transfer and porous medium" Physics Letters A 372 (2008) 4586–4591.

[3] C.Uma Devi; YVK.RAVI KUMAR; Tahmeena Kawkab" Investigation Of Jefferey Nanofluid Through An Inclined Tube With Permeable Walls" Journal of Xi'an University of Architecture & Technology ISSN No : 1006-7930 (2020).

[4] N. Subadra and K. Maruthi Prasad and S. Ravi Prasad Rao" Influence of Slip and Heat and Mass Transfer Effects on Peristaltic motion of Power-law fluid Prone to the Tube" Journal of Physics: Conference Series 1495 (2020) 012039.

[5] Saif Razzaq Mohsin Al-Waily ; Dheia G. Salih Al-Khafajy" Effect of wall properties on the peristaltic flow of a couple – Stress for Jeffrey fluid" AIP Conference Proceedings 2398, 060079 (2022)

[6] Dheia GS Al-khafajy, Ahmed Abd Alhadi. Magnetohydrodynamic Peristaltic flow of a couple stress with heat and mass transfer of a Jeffery fluid in a tube through porous medium, Advances in Physics Theories and Applications, 2014, 32.

[7] Hayat T, Asghar S, Tanveer A, Alsaedi A. Chemical reaction in peristaltic motion of MHD couple stress fluid in channel with Soret and Dufour effects, Results in physics, 2018, 10, 69-80.

[8] Sankad GC, Nagathan PS. Transport of MHD couple stress fluid through peristalsis in a porous medium under the influence of heat transfer and slip effects. International journal of applied mechanics and engineering, 2017, 22(2), 403-414.

[9] Rahmat Ellahi, Ahmed Zeeshan, Farooq Hussain, Asadollahi A. Peristaltic blood flow of couple stress fluid suspended with nanoparticles under the influence of chemical reaction and activation energy. Symmetry, 2019, 11(2), 276.

[10] Samah F Jaber AL-khulaifawi, Dheia GS Al-Khafajy. MHD Peristaltic Flow of a Couple-Stress with varying Temperature for Jeffrey Fluid through Porous Medium, Journal of Physics: Conference Series, 2020, 1591 012075.

[11] Dheia G. Salih Al-Khafajy and Saif Razzaq Mohsin Al-Waily" Magnetohydrodynamics Peristaltic Flow of a Couple- Stress for a Jeffrey Fluid through a Flexible Porous Medium" 2021 J. Phys.: Conf. Ser. 1999 012105.